

Building an irreversible Carnot-like heat engine with an overdamped harmonic oscillator

Carlos A Plata¹, David Guéry-Odelin²,
Emmanuel Trizac³ and A Prados⁴

¹ Dipartimento di Fisica e Astronomia ‘Galileo Galilei’, INFN, Università di Padova, Via Marzolo 8, 35131 Padova, Italy

² Laboratoire Collisions, Agrégats, Réactivité, IRSAMC, Université de Toulouse, CNRS, UPS, Toulouse, France

³ Université Paris-Saclay, CNRS, LPTMS, 91405, Orsay, France

⁴ Física Teórica, Universidad de Sevilla, Apartado de Correos 1065, E-41080 Sevilla, Spain

E-mail: prados@us.es

Received 1 July 2020

Accepted for publication 19 August 2020


Published 22 September 2020

Online at stacks.iop.org/JSTAT/2020/093207
<https://doi.org/10.1088/1742-5468/abb0e1>



Abstract. We analyse non-equilibrium Carnot-like cycles built with a colloidal particle in a harmonic trap, which is immersed in a fluid that acts as a heat bath. Our analysis is carried out in the overdamped regime. The cycle comprises four branches: two isothermal processes and two *locally* adiabatic ones. In the latter, both the temperature of the bath and the stiffness of the harmonic trap vary in time, but in such a way that the average heat vanishes for all times. All branches are swept at a finite rate and, therefore, the corresponding processes are irreversible, not quasi-static. Specifically, we are interested in optimising the heat engine to deliver the maximum power and characterising the corresponding values of the physical parameters. The efficiency at maximum power is shown to be very close to the Curzon–Ahlborn bound over the whole range of the ratio of temperatures of the two thermal baths, pointing to the near optimality of the proposed protocol.

Keywords: stochastic thermodynamics, dynamical processes

 Supplementary material for this article is available [online](#)

Contents

1. Introduction	2
2. The model system	4
2.1. Definition	4
2.2. Non-dimensional variables	6
3. Building blocks of the cycle: isothermal and adiabatic processes	6
3.1. Isothermal processes	7
3.2. Adiabatic processes	8
4. Irreversible Carnot-like heat engine	9
4.1. Quasi-static case	10
4.2. Irreversible Carnot-like cycle at finite speed	10
5. Efficiency at maximum power and the Curzon–Ahlborn bound	14
5.1. Maximal power at fixed temperature and compression ratios	14
5.2. Maximal power for fixed temperature ratio	16
6. Conclusions	17
Acknowledgments	18
References	18

1. Introduction

The investigation of heat engines is a pillar of classical thermodynamics [1]. The practical interest of the conversion of thermal energy into mechanical work led to unravel the laws of thermodynamics. These laws have been well formulated since the 19th century for macroscopic systems, for which fluctuations are negligible. In this context, the Carnot heat engine has played a major role: the Carnot cycle comprises two isothermal and two adiabatic branches, which are swept in a quasi-static, reversible, way. This *reversible Carnot heat engine* maximises the efficiency but the infinite time operation entails that the delivered power vanishes. In the adiabatic branches, the system is thermally isolated from the bath and there is no heat exchange—moreover, reversibility implies that there is no entropy variation either.

The extension of thermodynamic results to mesoscopic systems, where fluctuations are of paramount importance, is not straightforward; stochastic thermodynamics has been developed to this end [2–4], the focus of which lies on non-equilibrium dynamics. In recent years, researchers have looked into the possibility of speeding up the relaxation of physical systems between two given equilibrium states [5–11]. The emerging ‘engineered swift equilibration’ (ESE) [5, 6, 8, 9] and ‘shortcuts to isothermality’ (STI) [7, 10, 11] techniques, which are closely related but not equivalent in general, can be viewed as the

counterpart in the classical realm of the quantum ‘shortcuts to adiabaticity’ (STA) [12]. Anyway, STA, STI, and ESE processes make it possible to connect given initial and target states in a time that is much shorter than the natural characteristic relaxation time of the system at hand. To avoid confusion, it is perhaps worthwhile pointing that ‘adiabaticity’ in STA refers to a slow variation and not to the absence of heat transfer, at variance with terminology to be used below.

STA, STI, and ESE techniques make it possible to build heat engines that connect equilibrium states in a finite time, i.e. in an irreversible way. Therefore, the irreversible counterparts of the classical heat engines can be constructed at the mesoscopic level. In fact, our main goal is building an irreversible version of the Carnot heat engine with a colloidal particle in a harmonic trap of stiffness k , immersed in a fluid at equilibrium with temperature T . This system is relevant from both the theoretical and experimental standpoints. However, a difficulty arises: for mesoscopic systems, it is impossible to completely decouple the system from the heat bath to thermally isolate it—the interaction between a Brownian particle and the fluid in which it is immersed cannot be switched off. Moreover, zero heat and no entropy increment are not equivalent for finite time processes.

The above discussion entails that the definition of adiabatic—in the thermodynamical sense—process is far from trivial at the mesoscale. Notwithstanding, very recently, *finite-time adiabatic processes* have been characterised for a wide class of mesoscopic systems [13], in the overdamped description of the dynamics. In these processes, the average heat vanishes for all times but there is entropy creation, as imposed by the second principle. We employ these finite-time adiabatic processes to build the corresponding adiabatic branches of the irreversible Carnot engine. Therefore, our approach differs from other recent attempts to construct an irreversible Carnot engine [14–18], the limitations of which are discussed in what follows. Specifically, we focus on the respective definitions of ‘adiabaticity’. In reference [14], working in the overdamped regime, the term adiabatic has been employed for a process in which the bath temperature T is instantaneously changed, while the configurational distribution is frozen. However, as already noted by the authors of that work, neither heat nor the entropy increment vanishes in such a process, which are thus non-adiabatic, because of the kinetic contribution thereto. In references [15, 17, 18], the adiabatic branches are constructed by changing both the temperature of the bath and the stiffness k of the trap but keeping the ratio T^2/k constant, which is obtained in the underdamped description. Nevertheless, the condition $T^2/k = \text{const.}$ has been shown to correspond to isoentropic processes only in the quasi-static limit [15, 19], so such a process is not adiabatic either for finite time operation⁵. A completely different approach is proposed in reference [16]. Therein, the oscillator follows a Hamiltonian dynamics and is completely decoupled from the heat bath during the adiabatic branches, a procedure that cannot be implemented with a Brownian particle immersed in a fluid.

The performance of a heat engine is characterised by its efficiency and power. The maximum efficiency achievable operating between a hot bath at temperature T_h and a

⁵Reference [13], although working in the overdamped description, incorporates the kinetic contribution to the energy balance. Therein, the ratio T^2/k has been shown to be a non-decreasing function of time for finite-time adiabatic processes, being constant only in the quasi-static limit.

cold bath at temperature T_c is the well-known Carnot efficiency $\eta_C = 1 - T_c/T_h$. However, it is reached for infinite time operation, which makes the power vanish⁶. The cycle must be swept in a finite time to yield a nonzero power output. This acceleration of the process entails a non-equilibrium dynamics and reduces the reachable efficiency. The study of efficiency at maximum power is a classical problem associated with the field of finite-time thermodynamics [24–29]. Curzon and Ahlborn derived that the efficiency at maximum power for a macroscopically endoreversible heat engine is given by $\eta_{CA} = 1 - \sqrt{T_c/T_h}$ [24].

There is no general proof ensuring that the efficiency of any arbitrary heat engine at maximum power is bounded by the Curzon–Ahlborn value. Nevertheless, myriads of different studies hint at the existence of some universal properties, connected to the Curzon–Ahlborn bound, for the efficiency at maximum power. Specifically, it has been proven that in the limit of small relative temperature difference, the two first terms in the expansion of the efficiency at maximum power in the Carnot efficiency are universal [30–32]. This finding is completely consistent with the results for the efficiency at maximum power in different stochastic heat engines constructed either with a Brownian particle [14], a Feynman ratchet [33], or a quantum dot [34].

Another main objective of our work is the optimisation of the irreversible Carnot engine. Specifically, in connection with the discussion above, we are interested in looking into the optimisation in a sense to be specified soon below, of the delivered power and its associated efficiency. In this regard, the optimal protocols for isothermal and the adiabatic branches, which have been explicitly worked out recently [13, 14, 35, 36], play a crucial role. It appears that work should be minimised in the isothermal processes [14, 35, 36], whereas the connection time is minimised in the adiabatic ones [13].

The rest of the paper is organised as follows. In section 2, we introduce the model system with which we construct our heat engine: a Brownian particle moving in a harmonic trap. Special attention is paid to its energetics. Section 3 is devoted to putting forward the optimal protocols for both the isothermal and adiabatic branches. These protocols allow us to build the Carnot-like cycle, which is analysed in section 4. The efficiency at maximum power is thoroughly investigated in section 5. In section 6, the main conclusions of our work are presented. Finally, we refer to the supplementary material (<http://stacks.iop.org/JSTAT/2020/093207/mmedia>) for some further technical details, which complement the main text.

2. The model system

2.1. Definition

We consider a one-dimensional (1D) overdamped harmonic oscillator of stiffness k in contact with a thermal bath at temperature T . A Brownian particle, confined by optical tweezers, provides an accurate realisation. The stochastic dynamics of the system may be modelled at either the Langevin or the Fokker–Planck levels of description. Namely,

⁶Recently, it has been suggested that the Carnot efficiency can also be achieved in the opposite ‘infinitely fast’ limit in certain situations [20–23].

the Langevin equation for the position x of the oscillator reads

$$\lambda \frac{dx(t)}{dt} = -k(t)x(t) + \zeta(t), \quad (1)$$

where λ is the friction coefficient and ζ is a Gaussian white noise force, such that

$$\langle \zeta(t) \rangle = 0, \quad \langle \zeta(t)\zeta(t') \rangle = 2\lambda k_B T(t) \delta(t - t'), \quad (2)$$

with k_B and T being the Boltzmann constant and the temperature of the bath respectively. Physically, we are considering that the harmonic oscillator is immersed in a certain fluid that plays the role of the heat bath, which provides the values of the temperature T and the friction coefficient λ . Throughout our work, we take λ as constant⁷, time-independent, but we assume both the stiffness of the oscillator k and the bath temperature T to be externally controlled. While the time control of trap stiffness is now routinely achieved experimentally, we refer to references [4, 37] for the time control of temperature.

The evolution equation for the average variance of the oscillator $\langle x^2 \rangle$ can be straightforwardly derived from the Langevin equation (1), yielding

$$\lambda \frac{d\langle x^2 \rangle}{dt} = -2k \langle x^2 \rangle + 2k_B T. \quad (3)$$

At any time t , the state of the system is characterised by the state-point $(k, \langle x^2 \rangle, T)$. Equilibrium states fulfil the *equation of state* $\langle x^2 \rangle_{\text{eq}} = k_B T/k$. The above relation, which has been obtained by making the rhs of equation (3) vanish, defines the equilibrium surface in the $(k, \langle x^2 \rangle, T)$ three-dimensional space. We want to describe the energetics of this system at the average level. Thus we define the average energy

$$E = \frac{1}{2}k \langle x^2 \rangle + \frac{1}{2}k_B T, \quad (4)$$

where we have taken into account that the velocity variable is always at equilibrium in the overdamped limit. The equilibrium value of the energy is then $E_{\text{eq}} = k_B T$.

Let us now consider a process starting from a certain state A and ending in another state B . Work and heat are defined by the relations [2]

$$W_{AB} = \frac{1}{2} \int_A^B \langle x^2 \rangle dk, \quad (5)$$

$$Q_{AB} = \frac{1}{2} \int_A^B (k d\langle x^2 \rangle + k_B dT) = \frac{1}{2} \int_A^B k d\langle x^2 \rangle + \frac{k_B}{2} (T_B - T_A), \quad (6)$$

where T_A and T_B are the temperature values for the initial and final states, A and B , respectively. Thus, the first law of thermodynamics reads $\Delta E \equiv E_B - E_A = W_{AB} + Q_{AB}$. We have used the following sign convention: for $W, Q > 0$ energy is transferred from the environment to the system, whereas for $W, Q < 0$ energy is transferred from the system to the environment, irrespective of the ‘kind’ of energy involved. Therefore,

⁷Indeed, when considering a colloidal particle in an optical trap, λ is rooted in the solvent viscosity and is essentially constant.

in order to consider a heat engine, we are interested in cycles with a negative total work.

2.2. Non-dimensional variables

First of all, we introduce dimensionless variables as follows: we divide the stiffness and the temperature by their respective initial values, $\kappa = k/k_0$, $\theta = T/T_0$, and the variance by its equilibrium value at the initial temperature, $y = \langle x^2 \rangle / \langle x^2 \rangle_{\text{eq},0} = k_0 \langle x^2 \rangle / (k_B T_0)$. Then, we have that $y(t=0) = 1$ if the system starts from an equilibrium state. Second, a dimensionless time is defined as $s = k_0 t / \lambda$. With the above definitions, the evolution of the system in non-dimensional variables is governed by

$$\frac{dy}{ds} = -2\kappa y + 2\theta, \quad (7)$$

where the equilibrium surface (or equation of state) reads,

$$\kappa y_{\text{eq}} = \theta. \quad (8)$$

Regarding the energetics, we introduce the dimensionless energy by dividing E by the equilibrium value at the initial time, $k_B T_0$. Consistently, non-dimensional work and heat are defined with the same energy unit, that is,

$$\mathcal{E} = \frac{1}{2}\kappa y + \frac{1}{2}\theta, \quad (9)$$

$$\mathcal{W}_{AB} = \frac{1}{2} \int_A^B y \, d\kappa, \quad \mathcal{Q}_{AB} = \frac{1}{2} \int_A^B \kappa \, dy + \frac{1}{2} (\theta_B - \theta_A). \quad (10)$$

The first law reads $\Delta \mathcal{E} \equiv \mathcal{E}_B - \mathcal{E}_A = \mathcal{W}_{AB} + \mathcal{Q}_{AB}$, and the equilibrium value of the energy is $\mathcal{E}_{\text{eq}} = \theta$.

In dimensionless variables, the state of the system is characterised by the state-point (κ, y, θ) at any time s . For our purposes, it is useful to consider the movement of the projection of the state-point onto the (κ, y) plane. In particular, the work \mathcal{W} , as given by equation (10), is proportional to the area below the curve $(\kappa(s), y(s))$ swept by the system as time increases.

3. Building blocks of the cycle: isothermal and adiabatic processes

Herein, we aim at building an irreversible heat engine with the above described overdamped harmonic oscillator. Our heat engine operates cyclically between a ‘hot’ source, at dimensionless temperature θ_h , and a ‘cold’ source, at temperature $\theta_c < \theta_h$. Specifically, the non-equilibrium cycle comprises four different processes: two isothermal ones, at temperatures θ_h and θ_c , and two *locally* adiabatic ones that connect the isotherms. No heat is exchanged in average during these locally adiabatic processes at all times, as described below. This is the usual use of the term adiabatic in equilibrium thermodynamics, in which adiabatic is employed for a process in which the system is thermally insulated from the environment.

In each cycle, the engine takes energy from the hot reservoir as heat, $Q_h > 0$, and performs work, that is, $W < 0$. Therefore, the projection of the state-point onto the (κ, y) plane sweeps a certain closed curve $(\kappa(s), y(s))$, which characterises the considered cycle, in the counterclockwise direction. In the light of the above, isothermal and adiabatic processes can be considered as the *building blocks* for our irreversible heat engine. In the following, we summarise some results obtained in previous studies for isothermal [14, 36] and adiabatic processes [13].

3.1. Isothermal processes

We consider two kinds of isothermal processes at temperature θ : quasi-static and optimal. In both of them, the initial and final states characterised by (κ_A, y_B) and (κ_B, y_A) , respectively, correspond to equilibrium situations. Therefore, $\kappa_A y_A = \kappa_B y_B = \theta$.

First, we deal with the quasi-static case. Therein, κ is slowly tuned in such a way that the system sweeps the equilibrium curve $y(s) = \theta/\kappa(s)$ in the (κ, y) plane. Therefrom,

$$W = \frac{\theta}{2} \ln \frac{\kappa_B}{\kappa_A}, \quad Q = -W, \quad \Delta E = 0, \quad \mathcal{E}_B = \mathcal{E}_A = \theta. \quad (11)$$

Of course, this quasi-static process takes an infinite time.

Second, we look into the optimal process for a given finite time s_f . Therein, we are interested in the process for which the work performed by an external agent on the system is minimum, or in other words, we look for the maximum work produced by the system. The evolution of the variance in the optimal process is [14, 36].

$$\tilde{y}(s) = \left[\sqrt{y_A} + (\sqrt{y_B} - \sqrt{y_A}) \frac{s}{s_f} \right]^2. \quad (12)$$

From now, tilde denotes optimality in some sense: either for the profiles or for the values of the physical quantities or parameters. Note that $\tilde{y}(s)$ is continuous in the whole interval $[0, s_f]$.

The optimal evolution for the stiffness is obtained from the evolution equation (7) in the open interval $(0, s_f)$,

$$\tilde{\kappa}(s) = \frac{\theta}{\tilde{y}(s)} - \frac{1}{2} \frac{d}{ds} \ln \tilde{y}(s), \quad 0 < s < s_f. \quad (13)$$

We recall that the stiffness is discontinuous at both the initial and final times, $\tilde{\kappa}(s=0) = \kappa_A$, $\tilde{\kappa}(s=s_f) = \kappa_B$. In this problem, the elastic constant $\kappa(s)$ plays the role of the ‘control’ function in optimal control theory [38, 39]. Similar discontinuities in the ‘control’ function have been repeatedly found in stochastic thermodynamics [6, 14, 35, 36, 40–42].⁸

The optimal values of work and heat can also be readily calculated. The results are

$$\widetilde{W} = \frac{\theta}{2} \ln \frac{\kappa_B}{\kappa_A} + \frac{\theta}{s_f} \left(\frac{1}{\sqrt{\kappa_B}} - \frac{1}{\sqrt{\kappa_A}} \right)^2, \quad \widetilde{Q} = -\widetilde{W}, \quad (14)$$

⁸This is a consequence of the corresponding ‘Lagrangian’ being linear in the ‘velocities’ [43], which is sometimes called the Miele problem [44].

Of course, in this isothermal process there is no energy change between the initial and final states $\Delta\mathcal{E} = 0$, $\mathcal{E}_B = \mathcal{E}_A = \theta$. Note, however, that the energy of the system does change in the intermediate times, $\mathcal{E}(s) \neq \theta$ for $0 < s < s_f$ because we are dealing with a non-equilibrium process and $y(s) \neq \theta/\kappa(s)$, as expressed by equation (13).

3.2. Adiabatic processes

Now we turn our attention to adiabatic processes, there is no heat transfer at any point of the system trajectory. Therefore, bearing in mind equation (10) we have that the infinitesimal heat vanishes, i.e.

$$dQ \equiv \kappa dy + d\theta = 0, \tag{15}$$

Note that temperature becomes a function of time that goes from θ_A to θ_B in adiabatic processes. Similarly to the case of isothermal processes, we only consider adiabatic processes connecting two equilibrium states and then $\kappa_A y_A = \theta_A$, $\kappa_B y_B = \theta_B$.

The energetics of adiabatic processes is quite simple. The energy change is given by the change in temperature, $\mathcal{E}_A = \theta_A$, $\mathcal{E}_B = \theta_B$, $\Delta\mathcal{E} = \theta_B - \theta_A$. Since there is no heat exchange, $Q = 0$, work coincides with the energy change, $W = \theta_B - \theta_A$. The above expressions for energy, heat and work apply for any adiabatic process, regardless of its duration, and therefore are valid for both quasi-static and non-equilibrium processes. Nevertheless, the equivalence between adiabatic and isentropic processes occurs only in the quasi-static limit. It is in the non-equilibrium case that we deviate from the proposals in references [15, 17].

Again we consider two kinds of processes: quasi-static and optimal. First, in the quasi-static case, κ and θ are tuned in an infinitely slow way to allow the system sweep the equilibrium curve (8). Combining equations (8) and (15), one gets

$$y(s) = \frac{y_A \theta_A}{\theta(s)} = y_A \sqrt{\frac{\kappa_A}{\kappa(s)}}. \tag{16}$$

Second, we investigate optimal adiabatic processes. Here, optimal means something different from the sense we used in the previous section. As already said above, the work value is fixed by the initial and target states and thus cannot be optimised. However, two arbitrary states cannot be connected by an adiabatic transformation, the following inequality

$$\frac{\theta(s)}{\theta_A} \geq \left(\frac{y(s)}{y_A} \right)^{-1}, \tag{17}$$

holds for all times [13]. Therefore, for the initial and final times,

$$\frac{\theta_B}{\theta_A} \geq \left(\frac{y_B}{y_A} \right)^{-1} \quad \text{or, equivalently,} \quad \left(\frac{\theta_B}{\theta_A} \right)^2 \geq \frac{\kappa_B}{\kappa_A} \tag{18}$$

must be fulfilled. The equality in equations (17) and (18) corresponds to the quasi-static case (16).

There exists a minimum time to carry out an adiabatic process [13], namely

$$\tilde{s}_f = \frac{(y_B - y_A)^2}{2(y_B\theta_B - y_A\theta_A)}. \quad (19)$$

This minimum time is reached for a protocol in which the variance and the temperature evolve according to

$$\tilde{y}(s) = y_A + (y_B - y_A)\frac{s}{\tilde{s}_f}, \quad \tilde{\theta}(s) = \frac{y_A\theta_A + (y_B\theta_B - y_A\theta_A)\frac{s}{\tilde{s}_f}}{y_A + (y_B - y_A)\frac{s}{\tilde{s}_f}}, \quad (20)$$

which are valid in the whole interval $[0, \tilde{s}_f]$. Therefore, both $\tilde{y}(s)$ and $\tilde{\theta}(s)$ are continuous functions of time, including the initial and final times. The stiffness is given by

$$\tilde{\kappa}(s) = -\left(\frac{d\tilde{y}(s)}{ds}\right)^{-1} \frac{d\tilde{\theta}(s)}{ds}, \quad 0 < s < \tilde{s}_f. \quad (21)$$

and $\tilde{\kappa}(s = 0) = \kappa_A$, $\tilde{\kappa}(s = \tilde{s}_f) = \kappa_B$.

The discontinuity at the boundaries of $\kappa(s)$ does not break the adiabatic character of the process: there is no *instantaneous* heat transfer at the initial and/or final times. Since both the variance y and the temperature θ are continuous at the boundaries, the integration of the differential of heat, as defined in equation (15), between $s = 0$ and $s = 0^+$ (or between $s = \tilde{s}_f^-$ and $s = \tilde{s}_f$) vanishes. On the contrary, there is an instantaneous contribution to the work at both boundaries.

4. Irreversible Carnot-like heat engine

The aim of this work is to study a (stochastic) thermodynamic cycle comprising the following processes: (i) isothermal expansion starting from $(\kappa_A, y_A, \theta_A)$ up to $(\kappa_B, y_B, \theta_B = \theta_A)$ in contact with a hot bath at temperature θ_A , (ii) adiabatic expansion starting from $(\kappa_B, y_B, \theta_B = \theta_A)$ up to $(\kappa_C, y_C, \theta_C)$, (iii) isothermal compression starting from $(\kappa_C, y_C, \theta_C)$ up to $(\kappa_D, y_D, \theta_D = \theta_C)$ in contact with a cold bath at temperature θ_C , and (iv) adiabatic compression going from $(\kappa_D, y_D, \theta_D = \theta_C)$ to $(\kappa_A, y_A, \theta_A)$. We always choose the normalisation constants (units) such that $(\kappa_A, y_A, \theta_A) = (1, 1, 1)$.

As a consequence of the above processes being isothermal/adiabatic, we have the following general identities, $\mathcal{W}_{AB} = -\mathcal{Q}_{AB}$, $\mathcal{W}_{BC} = \mathcal{E}_C - \mathcal{E}_B = \theta_C - \theta_A$, $\mathcal{Q}_{BC} = 0$, $\mathcal{W}_{CD} = -\mathcal{Q}_{CD}$, $\mathcal{W}_{DA} = \mathcal{E}_A - \mathcal{E}_D = \theta_A - \theta_C = -\mathcal{W}_{BC}$, $\mathcal{Q}_{DA} = 0$. We focus on a heat engine, that is, a device that extracts heat from the hot bath and performs work, i.e.

$$\mathcal{Q}_{AB} = -\mathcal{W}_{AB} > 0, \quad \mathcal{W}_{AB} + \mathcal{W}_{BC} + \mathcal{W}_{CD} + \mathcal{W}_{DA} = \mathcal{W}_{AB} + \mathcal{W}_{CD} < 0. \quad (22)$$

The efficiency of such a device is defined by

$$\eta \equiv \frac{-(\mathcal{W}_{AB} + \mathcal{W}_{CD})}{\mathcal{Q}_{AB}} = 1 - \frac{\mathcal{W}_{CD}}{\mathcal{Q}_{AB}} < 1, \quad (23)$$

Table 1. Operating points of the Carnot engines. Panels (a) and (b) correspond to the reversible and irreversible versions, respectively.

(a)	κ	y	θ	(b)	κ	y	θ
A	1	1	1	A	1	1	1
B	χ	χ^{-1}	1	B	χ	χ^{-1}	1
C	$\nu^2\chi$	$\nu^{-1}\chi^{-1}$	ν	C	$c\nu^2\chi$	$c^{-1}\nu^{-1}\chi^{-1}$	ν
D	ν^2	ν^{-1}	ν	D	$d\nu^2$	$d^{-1}\nu^{-1}$	ν

whereas the power that delivers is given by

$$\mathcal{P} \equiv \frac{-(\mathcal{W}_{AB} + \mathcal{W}_{CD})}{s_{AB} + s_{BC} + s_{CD} + s_{DA}}, \tag{24}$$

where s_{AB} is the time employed for going from A to B , and so on.

4.1. Quasi-static case

First, we concentrate on the quasi-static limit, that is, we consider a Carnot cycle in which the harmonic oscillator is always at equilibrium. In principle, we must give 12 numbers to characterise the four operating points of the cycle (A, B, C, D), but we have the following constraints: (i) due to normalisation, state A is given, $(\kappa_A, y_A, \theta_A) = (1, 1, 1)$ (3 constraints), (ii) points (B, C, D) are equilibrium states (3 constraints), (iii) two isothermal relations $A-B$ and $C-D$ (2 constraints), and (iv) two adiabatic relations $B-C$ and $D-A$ (2 constraints). So, we need only $12 - 3 - 3 - 2 - 2 = 2$ variables to univocally define the quasi-static cycle.

The cycle is thus completely characterised by the temperature ratio ν and the compression ratio along the first isotherm χ . The values of the state variables (κ, y, θ) at the operating points of the cycle are collected in panel (a) of table 1. Note that the isotherm condition implies that $y_B/y_A = \kappa_A/\kappa_B = \chi^{-1}$, so the parameter χ certainly gives the compression ratio along the first isotherm. Hereafter, to keep our wording simpler, we call χ the compression ratio.

The efficiency of a Carnot cycle

$$\eta_C = 1 - \frac{\theta_C}{\theta_A} = 1 - \nu, \tag{25}$$

is well known and can be derived for any system without the knowledge of its state equation through entropic considerations [1]. Here, it can also be explicitly checked by calculating work and heat over the branches of the cycle. The power delivered by this engine is zero, because the processes are quasi-static and thus involve an infinite time.

4.2. Irreversible Carnot-like cycle at finite speed

Now we consider a similar cycle, being the only difference that the processes are carried out in a finite time and are thus irreversible. The adiabaticity of the second and third

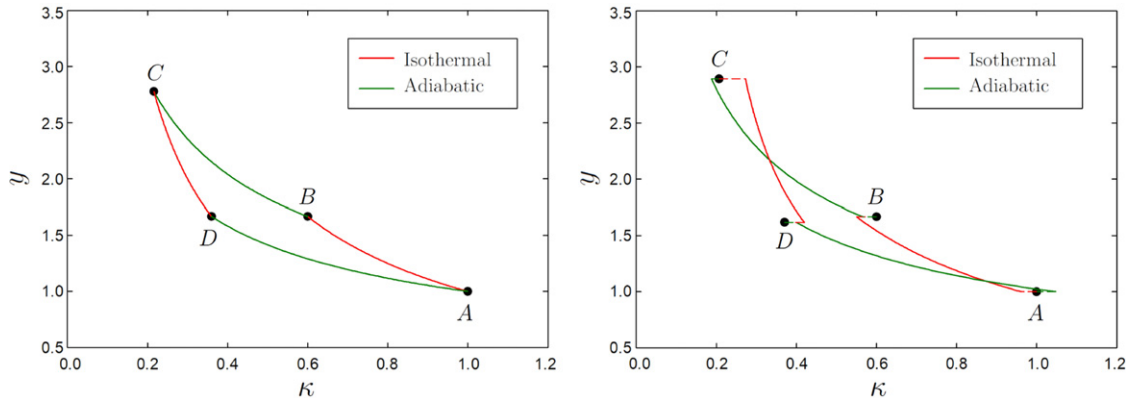


Figure 1. (a) Projection of the movement of the state-point onto the (κ, y) plane for a reversible Carnot engine. (b) Projection of the movement of the state-point onto the (κ, y) plane for an irreversible Carnot-like engine. Specifically, we have used the parameter values $\nu = 0.6$, $\chi = 0.6$, $c = 0.96$, $d = 1.03$ and the corresponding optimal protocols discussed in the text. In both plots, red lines correspond to the isothermal processes and green lines to the adiabatic ones. The dashed segments mark the jumps in the stiffness at the initial and final points of each of the four branches of the cycle.

process impose two inequalities, as expressed by equation (18). Therefore, we have that

$$\frac{\theta_C^2}{\theta_B^2} \geq \frac{\kappa_C}{\kappa_B}, \quad \frac{\theta_A^2}{\theta_D^2} \geq \frac{\kappa_A}{\kappa_D}, \quad (26)$$

which become equalities only for reversible processes, as those in the previous section. Thus, we need two additional parameters to define the cycle unambiguously, specifically we choose to introduce

$$c = \kappa_C \nu^{-2} \chi^{-1} \leq 1, \quad d = \kappa_D \nu^{-2} \geq 1, \quad (27)$$

which assure that equation (26) is fulfilled. In panel (b) of table 1, we summarise the values of the state variables (κ, y, θ) at the operating points of this non-equilibrium cycle. A comparative plot of the reversible and irreversible Carnot engines is shown in figure 1.

In the following, we focus our attention on the maximisation of the power delivered by the engine. Therefore, we build the heat engine that operates at maximum power for fixed operating points (A, B, C, D) or, equivalently, for given values of (ν, χ, c, d) . We approach the problem of the maximisation of the power defined in equation (24) in a stepwise manner. As discussed in detail below, the main idea is that the global maximum of \mathcal{P} can be obtained as the maximum of maximums, that is, we start by maximising with respect to some parameters keeping the remainder fixed. Afterwards, this maximum can be in turn be maximised with respect to the previously fixed parameters. For instance, maximisation can be performed for a given set $(\nu, \chi, c$ and $d)$, or in a more global fashion, specifying ν only.

Maximising equation (24) implies to take the shortest possible adiabatic protocols and the minimal work for the isothermal processes. This is readily understood as follows. The only dependence on the adiabatic protocols comes from s_{BC} and s_{DA} , so they have to be minimum in order to give the maximum value for \mathcal{P} . With respect to the isothermal processes, for fixed values of s_{AB} and s_{CD} , we have to maximise the respective work values $-\mathcal{W}_{AB}$ and $-\mathcal{W}_{CD}$, that is, minimise \mathcal{W}_{AB} and \mathcal{W}_{CD} . Therefore, we end up with the *optimal* processes, either isothermal or adiabatic, discussed in section 3. Making use of equations (12) and (13) for the isothermal processes and equations (19)–(21) for the adiabatic ones, we get

$$\mathcal{W}_{AB} = \frac{1}{2} \ln \chi + \frac{1}{s_{AB}} \left(\frac{1}{\sqrt{\chi}} - 1 \right)^2, \quad \mathcal{Q}_{AB} = -\mathcal{W}_{AB}, \quad (28)$$

$$\mathcal{W}_{CD} = -\frac{\nu}{2} \ln \frac{c\chi}{d} + \frac{1}{\nu s_{CD}} \left(\frac{1}{\sqrt{c\chi}} - \frac{1}{\sqrt{d}} \right)^2, \quad \mathcal{Q}_{CD} = -\mathcal{W}_{CD}, \quad (29)$$

$$\tilde{s}_{BC} = \frac{(1 - c\nu)^2}{2c\chi\nu^2(1 - c)}, \quad \tilde{s}_{DA} = \frac{(d\nu - 1)^2}{2d\nu^2(d - 1)} \quad (30)$$

It is worth commenting some points before proceeding further. On the one hand, \mathcal{W}_{CD} is always positive and thus \mathcal{Q}_{CD} is negative; isothermal compression work has to be done on the system and heat is always transferred from the device to the cold bath. On the other hand, in the isothermal expansion, \mathcal{W}_{AB} is negative for large enough s_{AB} , but \mathcal{W}_{AB} becomes positive if we intend to compress the system too fast: we have to exert work on the system in that case and moreover \mathcal{Q}_{AB} becomes negative and heat is transferred from the system to the hot bath. Therefore, we are not interested here in these too fast isothermal expansions because we would not be building a heat engine in that case. Below we show that this poses no problem because (i) the optimal value \tilde{s}_{AB} yields a negative value of \mathcal{W}_{AB} and (ii) the optimal value \tilde{s}_{CD} makes that $\mathcal{W}_{CD} < -\mathcal{W}_{AB}$, that is, $\mathcal{W}_{CD} + \mathcal{W}_{AB} < 0$. Thus, the heat engine conditions are met.

Let us build on the ideas above. We must impose the inequalities (22) to have a heat engine. In particular, these inequalities should hold when s_{AB} and s_{CD} go to infinity (reversible isotherms). It is useful to introduce the definitions

$$\mathcal{W}_1 \equiv \lim_{s_{AB} \rightarrow \infty} \mathcal{W}_{AB} = \frac{1}{2} \ln \chi < 0, \quad \mathcal{W}_2 \equiv \lim_{s_{CD} \rightarrow \infty} \mathcal{W}_{CD} = -\frac{\nu}{2} \ln \frac{c\chi}{d} > 0, \quad (31)$$

where we have taken into account that $\chi < 1$, $c \leq 1$, $d \geq 1$, and

$$\mathcal{W}_\infty \equiv \mathcal{W}_1 + \mathcal{W}_2 = \frac{1}{2} \ln \chi - \frac{\nu}{2} \ln \frac{c\chi}{d} < 0. \quad (32)$$

Although \mathcal{W}_1 coincides with the value of the work over the first isotherm in the fully reversible engine, neither \mathcal{W}_2 nor \mathcal{W}_∞ does because they depend on c and d . The negativeness of \mathcal{W}_∞ leads to the constraint

$$\frac{c}{d} > \chi^{\frac{1-\nu}{\nu}}. \quad (33)$$

Strictly speaking, this constraint has been shown to hold only in the limit as $s_{AB}, s_{CD} \rightarrow \infty$, but below we prove that it also holds for finite-time operation.

Therefore, we just have to maximise the power

$$\mathcal{P} = \frac{\frac{\nu-1}{2} \ln \chi + \frac{\nu}{2} \ln \frac{c}{d} - \frac{1}{s_{AB}} \left(\frac{1}{\sqrt{\chi}} - 1 \right)^2 - \frac{1}{\nu s_{CD}} \left(\frac{1}{\sqrt{d}} - \frac{1}{\sqrt{c\chi}} \right)^2}{s_{AB} + \tilde{s}_{BC} + s_{CD} + \tilde{s}_{DA}}, \quad (34)$$

with respect to s_{AB} and s_{CD} , by imposing that the partial derivatives of \mathcal{P} with respect to s_{AB} and s_{CD} vanish for the optimal durations of the isothermal processes⁹. In order to write the expressions for \tilde{s}_{AB} and \tilde{s}_{CD} , it is convenient to introduce the parameters

$$\Delta_1 = \sqrt{y_B} - \sqrt{y_A} = \frac{1}{\sqrt{\chi}} - 1 > 0, \quad (35)$$

$$\Delta_2 = \sqrt{y_D} - \sqrt{y_C} = \frac{1}{\sqrt{\nu}} \left(\frac{1}{\sqrt{d}} - \frac{1}{\sqrt{c\chi}} \right) < 0, \quad (36)$$

which measure the expansion and compression of the system in the first and second isotherms, respectively, and

$$\sigma = \sqrt{1 + \frac{(\tilde{s}_{BC} + \tilde{s}_{DA})(-\mathcal{W}_\infty)}{(\Delta_1 - \Delta_2)^2}} > 1. \quad (37)$$

As a function of these parameters, we can write now that

$$\tilde{s}_{AB} = \frac{\Delta_1(\Delta_1 - \Delta_2)(1 + \sigma)}{-\mathcal{W}_\infty}, \quad \tilde{s}_{CD} = \frac{-\Delta_2(\Delta_1 - \Delta_2)(1 + \sigma)}{-\mathcal{W}_\infty}. \quad (38)$$

The condition $\mathcal{W}_\infty < 0$ ensures the positivity of the optimal times.

Using the above definitions, we can write the work values for the optimal durations of the isothermal processes as

$$\tilde{\mathcal{W}}_{AB} = \mathcal{W}_1 + \frac{\Delta_1^2}{\tilde{s}_{AB}} = \frac{-\mathcal{W}_1\Delta_2 - \mathcal{W}_2\Delta_1 + \mathcal{W}_1\sigma(\Delta_1 - \Delta_2)}{(\Delta_1 - \Delta_2)(1 + \sigma)} < 0, \quad (39)$$

$$\tilde{\mathcal{W}}_{CD} = \mathcal{W}_2 + \frac{\Delta_2^2}{\tilde{s}_{CD}} = \frac{\mathcal{W}_1\Delta_2 + \mathcal{W}_2\Delta_1 + \mathcal{W}_2\sigma(\Delta_1 - \Delta_2)}{(\Delta_1 - \Delta_2)(1 + \sigma)} > 0. \quad (40)$$

By combining the expressions above, the total work in the cycle with the optimal durations is found to be

$$\tilde{\mathcal{W}}_{AB} + \tilde{\mathcal{W}}_{CD} = \frac{\sigma}{1 + \sigma} \mathcal{W}_\infty < 0. \quad (41)$$

The signs of $\tilde{\mathcal{W}}_{AB}$ and $\tilde{\mathcal{W}}_{AB} + \tilde{\mathcal{W}}_{CD}$ show that we have, in fact, a ‘good’ engine. Moreover, we get a physical interpretation for the parameter σ : it measures the deviation of the total irreversible work from the value for infinitely slow isothermal processes \mathcal{W}_∞ . In the limit as $\sigma \rightarrow \infty$, we have that $\tilde{\mathcal{W}}_{AB} + \tilde{\mathcal{W}}_{CD} \rightarrow \mathcal{W}_\infty$.

⁹Note that, since they do not depend on s_{AB} and s_{CD} , we have not substituted explicitly the values of \tilde{s}_{BC} and \tilde{s}_{DA} , given by equation (30), so as not to clutter the expression.

We have found the optimal values of the times for the isothermal and adiabatic protocols, for given values of the parameters (ν, χ, c, d) that univocally define the operating points of our irreversible Carnot-like heat engine. As a function of these parameters, the optimal power is thus given by

$$\tilde{\mathcal{P}} = \frac{-\mathcal{W}_\infty - \frac{\Delta_1^2}{\tilde{s}_{AB}} - \frac{\Delta_2^2}{\tilde{s}_{CD}}}{\tilde{s}_{AB} + \tilde{s}_{BC} + \tilde{s}_{CD} + \tilde{s}_{DA}} = \frac{-\mathcal{W}_\infty \frac{\sigma}{1+\sigma}}{\tilde{s}_{AB} + \tilde{s}_{BC} + \tilde{s}_{CD} + \tilde{s}_{DA}}, \quad (42)$$

Later, we address the issue of optimising the cycle further, by looking for the maximum of the $\tilde{\mathcal{P}}$ as a function of c, d and χ for a fixed value of the temperature ratio ν .

5. Efficiency at maximum power and the Curzon–Ahlborn bound

5.1. Maximal power at fixed temperature and compression ratios

Let us look into the the efficiency of the maximum power cycle,

$$\tilde{\eta} = -\frac{\tilde{\mathcal{W}}_{AB} + \tilde{\mathcal{W}}_{CD}}{\tilde{\mathcal{Q}}_{AB}} = 1 + \frac{\tilde{\mathcal{W}}_{CD}}{\tilde{\mathcal{W}}_{AB}}, \quad (43)$$

which depends on (ν, χ, c, d) . To keep our notation simple, either for $\tilde{\mathcal{P}}$ in equation (42) or $\tilde{\eta}$ in equation (43), we do not write explicitly the parameters which they depend on. This choice also applies to the remainder of the paper.

Making use of equation (39), we can rewrite $\tilde{\eta}$ as

$$\tilde{\eta} = \underbrace{1 - \nu}_{\eta_C} + \frac{(\nu - 1)(\mathcal{W}_1\Delta_2 + \mathcal{W}_2\Delta_1) - (\mathcal{W}_2 + \mathcal{W}_1\nu)\sigma(\Delta_1 - \Delta_2)}{\mathcal{W}_1\Delta_2 + \mathcal{W}_2\Delta_1 - \mathcal{W}_1\sigma(\Delta_1 - \Delta_2)} \quad (44)$$

All the terms in the denominator are clearly positive, whereas all the terms in the numerator are negative by taking into account that $\mathcal{W}_2 + \mathcal{W}_1\nu = -(\nu/2)\ln(c/d) > 0$. Therefore, $\tilde{\eta} < \eta_C$: the efficiency is always below the Carnot bound, as expected.

On the other hand, the comparison with the Curzon–Ahlborn bound [14, 24, 45, 46]

$$\eta_{CA} = 1 - \sqrt{\nu} \quad (45)$$

requires a more detailed analysis. Let us investigate two different cases. First, we consider values of the ratio c/d such that $\chi^{-1+\nu^{-1}} < c/d < \chi^{-1+\nu^{-1/2}}$, which entails that $\mathcal{W}_2 + \sqrt{\nu}\mathcal{W}_1 > 0$ and

$$\underbrace{(\sqrt{\nu} - 1)}_{<0} \underbrace{(\mathcal{W}_1\Delta_2 + \mathcal{W}_2\Delta_1)}_{>0} - \underbrace{(\mathcal{W}_2 + \mathcal{W}_1\sqrt{\nu})}_{>0} \underbrace{\sigma(\Delta_1 - \Delta_2)}_{>0} < 0. \quad (46)$$

In this region, a manipulation similar to the one done for showing that $\eta < \eta_C$ gives

$$\tilde{\eta} = 1 - \sqrt{\nu} + \frac{(\sqrt{\nu} - 1)(\mathcal{W}_1\Delta_2 + \mathcal{W}_2\Delta_1) - (\mathcal{W}_2 + \mathcal{W}_1\sqrt{\nu})\sigma(\Delta_1 - \Delta_2)}{\mathcal{W}_1\Delta_2 + \mathcal{W}_2\Delta_1 - \mathcal{W}_1\sigma(\Delta_1 - \Delta_2)}. \quad (47)$$

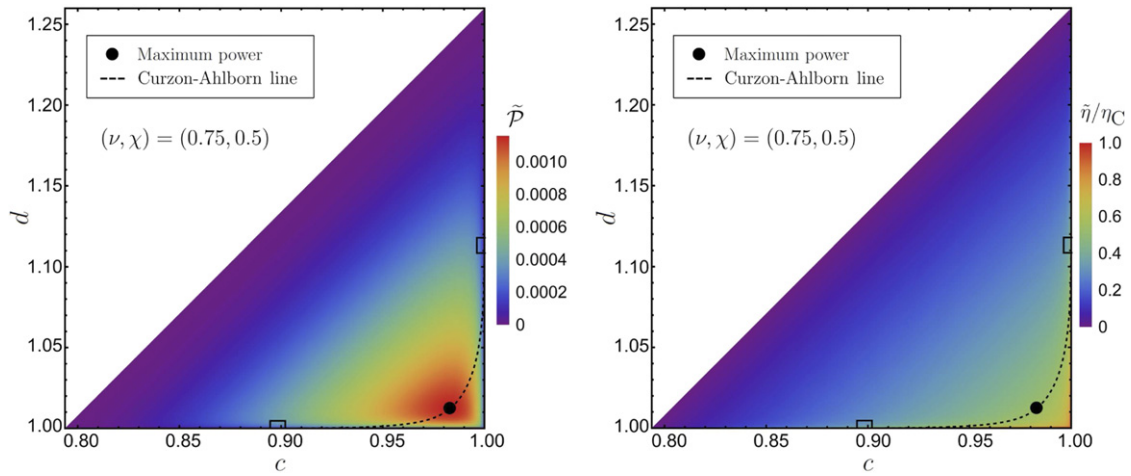


Figure 2. Density plots of the optimal power (left) and its corresponding efficiency (right) in the (c, d) plane. The curves where $\tilde{\eta} = \eta_{CA}$ (dashed line), with its initial and final points (open squares) over the axes $d = 1$ and $c = 1$, respectively, and the point at which the maximum power (circle) is reached, are displayed in both panels. We have taken $\nu = 0.75$ and $\chi = 0.5$.

Again, the denominator and the numerator are positive and negative respectively, which leads to the inequality $\tilde{\eta} < \eta_{CA}$. Nevertheless, for the complementary case, $\chi^{-1+\nu^{-1/2}} < c/d < 1$, we can no longer assure that the Curzon–Ahlborn is an upper bound. Indeed, in the double limit as $(c, d) \rightarrow (1, 1)$, we have that \tilde{s}_{BC} and \tilde{s}_{DA} diverge for fixed $\nu < 1$. In that limit, not only do the adiabatic processes become quasi-static but also the isothermal ones, recovering the quasi-static Carnot engine introduced in section 4.1, with optimal efficiency $\lim_{(c,d) \rightarrow (1,1)} \tilde{\eta} = \eta_C$. Because of continuity, we can always find values of c and d , given a value of χ , such that the efficiency of our optimal heat engine is arbitrarily close to the Carnot value and thus greater than the Curzon–Ahlborn bound. However, it has to be taken into account that the optimal power for this case is very small, because the denominator in equation (42) diverges. In section 1 of the supplementary material, we consider the leading order of $\tilde{\eta}$ and $\tilde{\mathcal{P}}$.

To illustrate the above results, we present in figure 2 a density plot of the optimal power, equation (42), and the corresponding efficiency, equation (43), as a function of c and d . Specifically, we consider given values of the temperature ratio $\nu = 0.75$ and the compression ratio $\chi = 0.5$. The constraint (33) entails that the meaningful region in the plane (c, d) is a right triangle of vertices $(c_{\min} = \chi^{\frac{1-\nu}{\nu}}, 1)$, $(1, 1)$ and $(1, d_{\max} = c_{\min}^{-1})$. Within this region, we can define another right triangle with the right angle in the same vertex and the hypotenuse given by the line $d = \chi^{\frac{\sqrt{\nu}-1}{\sqrt{\nu}}} c$, above which we know that $\tilde{\eta} < \eta_{CA}$. Below the aforementioned line, we cannot assure that $\tilde{\eta} < \eta_{CA}$ and in the limit as $(c, d) \rightarrow (1, 1)$ we know that $\tilde{\eta} \rightarrow \eta_C$. The curve over which $\tilde{\eta} = \eta_{CA}$, which departs from the hypotenuse vertices (open squares) of this second triangle and is fully contained within it, has been evaluated numerically and plotted (dashed line) along with the point of delivery of maximum power (circle).

There are several implications that can be drawn from this analysis. First, along all the sides of the delimiting triangle, the maximum power is zero because some of the optimal times diverge. Second, as a consequence of the previous point and the positiveness of $\tilde{\mathcal{P}}$, there always appears a maximum of the optimal power as a function of (c, d) (for fixed ν and χ), at a certain point \tilde{c}, \tilde{d} . Third, the numerical estimate for this maximum is very close to the dotted line, at which $\tilde{\eta} = \eta_{CA}$. This last observation is especially robust for either small χ or large ν , as can be seen in section 2 of the supplementary material, in which analogous plots for different couples of values (ν, χ) are presented.

5.2. Maximal power for fixed temperature ratio ν

The numerical analysis shown in figure 2 suggests that studying further the maximum power that can be achieved for fixed values of ν and χ , that is, as a function of c and d , may be illuminating. This is a meaningful physical question: recall that the reversible Carnot engine is completely determined by these two parameters. Moreover, its efficiency η_C does not depend on the compression ratio χ , which makes interesting even a further maximisation in the compression ratio χ .

It is possible to address this problem by maximising again the optimal power in equation (42) with respect to c and d , and finally with respect to χ . Doing so analytically is not feasible since it involves transcendental equations. Nevertheless, a systematic asymptotic analysis can be carried out for $\nu \rightarrow 1$. In this regime, the main idea is to expand all the physical quantities in powers of $\eta_C = 1 - \nu$. In order to avoid cluttering the information flow with the technicalities of the asymptotic analysis, we present the detailed calculation in sections 3 and 4 of the supplementary material. Therein, it is shown that the expansions of $\tilde{\mathcal{P}}$ and $\tilde{\eta}$ in the Carnot efficiency up to order η_C^4 and η_C^3 , respectively, are

$$\tilde{\mathcal{P}} = \frac{\eta_C^2}{16} - \frac{\eta_C^{5/2}}{8} + \frac{5}{48}\eta_C^3 - \frac{11}{144}\eta_C^{7/2} + \frac{937}{17280}\eta_C^4 + O(\eta_C^{9/2}), \quad (48)$$

$$\tilde{\eta} = \frac{\eta_C}{2} + \frac{\eta_C^2}{8} + \frac{\eta_C^3}{32} + O(\eta_C^{7/2}). \quad (49)$$

We recall that the expansion of the Curzon–Ahlborn efficiency is

$$\eta_{CA} = \frac{\eta_C}{2} + \frac{\eta_C^2}{8} + \frac{\eta_C^3}{16} + O(\eta_C^4), \quad (50)$$

Similarly to the situation reported in references [14, 34] the first two terms in the expansion of $\tilde{\eta}$ in powers of η_C coincide with those in η_{CA} and the deviation occurs in the third term, of the order of $O(\eta_C^3)$. The obtained efficiency at maximum power is smaller than the Curzon–Ahlborn bound, similarly to the situation found in reference [14].¹⁰

In figure 3, we plot the efficiency at maximum power as a function of ν . Power has been numerically maximised over c, d and χ . The obtained efficiency $\tilde{\eta}$ is compared

¹⁰See equations (24) and (25) in that paper. However, the reverse situation has also been found, see for instance equation (20) in reference [34].

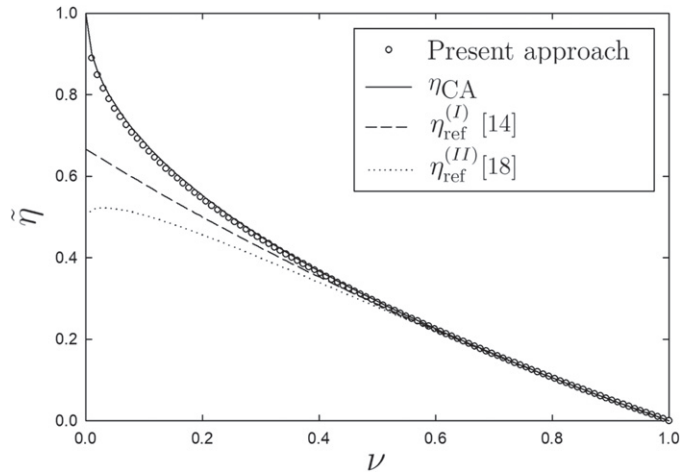


Figure 3. Efficiency at maximum power as a function of the temperature ratio ν . The value obtained for the efficiency, once that the optimisation of the power is numerically performed for the rest of parameters, is almost indistinguishable from the Curzon–Ahlborn bound η_{CA} . Our construction develops a better efficiency compared with those shown in references [14, 18].

with (i) the Curzon–Ahlborn bound, (ii) the efficiency for the engine with instantaneous ‘adiabatic’ branches developed in [14], $\eta_{\text{ref}}^{(I)} = 2\eta_C/(4 - \eta_C)$, and (iii) the efficiency obtained for large dissipation in the recent proposal, using a fast forward approach [18], to build a Carnot-like engine, $\eta_{\text{ref}}^{(II)} = (1 - \nu)(1 + \sqrt{\nu})/[2 + \sqrt{\nu}(1 + \nu)] \leq \eta_{\text{ref}}^{(I)}$. It is clearly observed that $\tilde{\eta} \geq \eta_{\text{ref}}^{(I)}$ for all ν , with the difference between them increasing as ν decreases. Moreover, the closeness between the efficiency of our engine at maximum power and the Curzon–Ahlborn bound goes beyond our expectations based on the asymptotic analysis, holding not only within the limit $\nu \rightarrow 1$ but also for the whole range of ν . Specifically, the relative deviation between our numerical values for efficiency at maximum power and the Curzon–Ahlborn bound always remains under 2%. Therefore, our novel irreversible Carnot-like heat engine is certainly a very efficient one at maximum power.

6. Conclusions

In this work, we have put forward an irreversible Carnot-like heat engine that can be experimentally implemented with a colloidal particle immersed in a fluid. Our model system is a Brownian particle trapped in a harmonic potential, in the overdamped regime. The adiabatic branches of the proposed cycle are *truly adiabatic* in the classical thermodynamic sense: at every point thereof, there is no heat exchange with the thermal bath. Of course, the heat exchange vanishes in average: it is impossible to completely decouple the colloidal particle from the surrounding fluid. Therefore, our locally adiabatic branches contrast with the approach followed in other works, in which the system has a non-vanishing heat exchange in the ‘adiabatic’ parts of the cycle [4, 14, 17, 19].

The cycle of the reversible Carnot heat engine is completely characterised by the temperature ratio ν and the compression ratio χ . For our irreversible counterpart of the Carnot heat engine, we need two more parameters in order to fully characterise the four operating points of the cycle: the adiabatic condition imposes restrictions on—but does not univocally define—the operating points.

We have thoroughly studied the performance of the Carnot-like heat engine at maximum power. We have adopted a step-by-step optimisation approach. First, the maximum power is shown to be obtained for the optimal protocols for both isothermal—maximum work [14, 35, 36]—and adiabatic—minimum duration [13]—branches. In a second step, we have optimised the power over the duration of the isothermal processes. These two stages of the optimisation have been carried out for fixed operation points in the state space (κ, y, T) —(stiffness, variance of position, temperature). Finally, we have maximised the power over the operation points by just fixing the temperature ratio ν .

The efficiency at maximum power for our heat engine is very close to the Curzon–Ahlborn bound. This behaviour is predicted by an asymptotic analysis for $\nu \rightarrow 1$. Nevertheless, we have numerically shown that this result remarkably holds for the whole range of temperature ratios, well beyond the asymptotic prediction. This implies that our cycle is a close to optimal choice for building an efficient mesoscopic heat engine, as compared with the theoretical predictions for other constructions [14, 18].

Possible venue for future work are discussed in the following. First, it is worth studying fluctuations, thus going beyond the mean scenario reported here [47–51]. Second, a universal trade-off relation between power and efficiency has recently been shown to hold for Markovian heat engines [52]. In this regard, it seems especially relevant to investigate the optimisation of the so-called ‘figures of merit’, which involve combinations of power and efficiency [53–56].

Acknowledgments

AP acknowledges financial support from the Spanish Agencia Estatal de Investigación through Grant PGC2018-093998-B-I00, partially financed by the European Regional Development Fund. CAP acknowledges the support from University of Padova through Project STARS-Stg (CdA Rep. 40, 23.02.2018) BioReACT grant. This work has also been financially supported by the Agence Nationale de la Recherche through Grant ANR-18-CE30-0013 (DG-O, ET).

References

- [1] Callen H 1985 *Thermodynamics and an Introduction to Thermostatistics* (New York: Wiley)
- [2] Sekimoto K 2010 *Stochastic Energetics* (Berlin: Springer)
- [3] Seifert U 2012 *Rep. Prog. Phys.* **75** 126001
- [4] Ciliberto S 2017 *Phys. Rev. X* **7** 021051
- [5] Martínez I A, Petrosyan A, Guéry-Odelin D, Trizac E and Ciliberto S 2016 *Nat. Phys.* **12** 843–6
- [6] Muratore-Ginanneschi P and Schwieger K 2017 *Entropy* **19** 379
- [7] Li G, Quan H T and Tu Z C 2017 *Phys. Rev. E* **96** 012144
- [8] Chupeau M, Ciliberto S, Guéry-Odelin D and Trizac E 2018 *New J. Phys.* **20** 075003

- [9] Chupeau M, Besga B, Guéry-Odelin D, Trizac E, Petrosyan A and Ciliberto S 2018 *Phys. Rev. E* **98** 010104
- [10] Albay J A C, Wulaningrum S R, Kwon C, Lai P Y and Jun Y 2019 *Phys. Rev. Res.* **1** 033122
- [11] Albay J A C, Lai P-Y and Jun Y 2020 *Appl. Phys. Lett.* **116** 103706
- [12] Guéry-Odelin D, Ruschhaupt A, Kiely A, Torrontegui E, Martínez-Garaot S and Muga J 2019 *Rev. Mod. Phys.* **91** 045001
- [13] Plata C A, Guéry-Odelin D, Trizac E and Prados A 2020 *Phys. Rev. E* **101** 032129
- [14] Schmiedl T and Seifert U 2008 *Europhys. Lett.* **81** 20003
- [15] Bo S and Celani A 2013 *Phys. Rev. E* **87** 050102
- [16] Tu Z C 2014 *Phys. Rev. E* **89** 052148
- [17] Martínez I A, Roldán É, Dinis L, Petrov D, Parrondo J M R and Rica R A 2016 *Nat. Phys.* **12** 67–70
- [18] Nakamura K, Matrasulov J and Izumida Y 2020 *Phys. Rev. E* **102** 012129
- [19] Martínez I A, Roldán E, Dinis L, Petrov D and Rica R A 2015 *Phys. Rev. Lett.* **114** 120601
- [20] Shiraishi N 2015 *Phys. Rev. E* **92** 050101
- [21] Campisi M and Fazio R 2016 *Nat. Commun.* **7** 11895
- [22] Lee J S and Park H 2017 *Sci. Rep.* **7** 10725
- [23] Poletini M and Esposito M 2017 *Europhys. Lett.* **118** 40003
- [24] Curzon F L and Ahlborn B 1975 *Am. J. Phys.* **43** 22–4
- [25] Andresen B, Salamon P and Berry R S 1977 *J. Chem. Phys.* **66** 1571–7
- [26] De Vos A 1985 *Am. J. Phys.* **53** 570–3
- [27] Hoffmann K H, Watowich S J and Berry R S 1985 *J. Appl. Phys.* **58** 2125–34
- [28] Chen L and Yan Z 1989 *J. Chem. Phys.* **90** 3740–3
- [29] Chen J 1994 *J. Phys. D: Appl. Phys.* **27** 1144–9
- [30] Van den Broeck C 2005 *Phys. Rev. Lett.* **95** 190602
- [31] Esposito M, Lindenberg K and Van den Broeck C 2009 *Phys. Rev. Lett.* **102** 130602
- [32] Sheng S and Tu Z C 2015 *Phys. Rev. E* **91** 022136
- [33] Tu Z C 2008 *J. Phys. A: Math. Theor.* **41** 312003
- [34] Esposito M, Lindenberg K and Van den Broeck C 2009 *Europhys. Lett.* **85** 60010
- [35] Schmiedl T and Seifert U 2007 *Phys. Rev. Lett.* **98** 108301
- [36] Plata C A, Guéry-Odelin D, Trizac E and Prados A 2019 *Phys. Rev. E* **99** 012140
- [37] Martínez I A, Roldán E, Parrondo J M R and Petrov D 2013 *Phys. Rev. E* **87** 032159
- [38] Pontryagin L S 1987 *Mathematical Theory of Optimal Processes* (Boca Raton: CRC Press)
- [39] Liberzon D 2012 *Calculus of Variations and Optimal Control Theory: A Concise Introduction* (Princeton: Princeton University Press)
- [40] Band Y B, Kafri O and Salamon P 1982 *J. Appl. Phys.* **53** 8–28
- [41] Aurell E, Mejía-Monasterio C and Muratore-Ginanneschi P 2011 *Phys. Rev. Lett.* **106** 250601
- [42] Aurell E, Mejía-Monasterio C and Muratore-Ginanneschi P 2012 *Phys. Rev. E* **85** 020103
- [43] Newman E and Bergmann P G 1955 *Phys. Rev.* **99** 587–92
- [44] Tolle H 2012 *Optimization Methods* (Berlin: Springer Science and Business Media)
- [45] Esposito M, Kawai R, Lindenberg K and Van den Broeck C 2010 *Phys. Rev. Lett.* **105** 150603
- [46] Apertet Y, Ouerdane H, Goupil C and Lecoeur P 2017 *Phys. Rev. E* **96** 022119
- [47] Gingrich T R, Rotskoff G M, Vaikuntanathan S and Geissler P L 2014 *New J. Phys.* **16** 102003
- [48] Poletini M, Verley G and Esposito M 2015 *Phys. Rev. Lett.* **114** 050601
- [49] Holubec V and Ryabov A 2018 *Phys. Rev. Lett.* **121** 120601
- [50] Gupta D 2018 *J. Stat. Mech.* **2018** 073201
- [51] Manikandan S K, Dabelow L, Eichhorn R and Krishnamurthy S 2019 *Phys. Rev. Lett.* **122** 140601
- [52] Shiraishi N, Saito K and Tasaki H 2016 *Phys. Rev. Lett.* **117** 190601
- [53] Holubec V and Ryabov A 2015 *Phys. Rev. E* **92** 052125
- [54] Holubec V and Ryabov A 2016 *J. Stat. Mech.* **2016** 073204
- [55] Ma Y H, Xu D, Dong H and Sun C P 2018 *Phys. Rev. E* **98** 042112
- [56] Abiuso P and Perarnau-Llobet M 2020 *Phys. Rev. Lett.* **124** 110606